

Research on Engineering Structures & Materials



www.jresm.org

Research Article

Development of lightweight cold-formed steel sections equivalent to hot-rolled profiles

Hadi Hasan Mussttaf a, Kawther K. Younus *,b

Abstract

Electrical Engineering Technical College, Middle Technical University, Baghdad, Iraq

Article Info

Article History:

Received 12 July 2025 Accepted 11 Oct 2025

Keywords:

Cold-formed steel; Structural performance; Finite element analysis; Lightweight steel Profiles; Sustainable steel construction This project demonstrates to develop and evaluate a new cold-formed HPE profile consisting of a C-profile with two web notches and one flange notch. Using an automated welding equipment, the profile is welded to two U-profiles with single notches in the web to produce a composite section with increased structural efficiency. This innovative design ensures the HPE profile is fully effective and puts the cold-formed profile on level with traditional IPE sections in terms of loadbearing capabilities, efficiency, and durability. Through material and shape optimization, the recommended profile greatly reduces weight while maintaining structural performance. Furthermore, by combining a notched cold-formed Cprofile with two welded U-profiles, this work presents a novel welded composite HPE profile that deviates from previously published built-up and hybrid coldformed sections. This arrangement permits manufacture through continuous rollforming and automated welding while optimizing local stiffness and material distribution. To clearly establish the originality and useful benefits of the proposed HPE section, a comparative synthesis of important geometric and performance parameters against representative built-up and hot-rolled profiles has been added (see Table 1). According to the study, as compared to equivalent IPE sections, the suggested HPE profiles were able to reduce weight by up to 35% while keeping load-bearing capacity same or even slightly greater (by up to 8%). These numerical results highlight the developed cold-formed profiles' structural and economic benefits. These advancements address the financial challenges caused by rising steel costs and encourage sustainable building practices by lowering resource consumption. This study offers a comprehensive evaluation of the recommended profile's structural behavior, effectiveness, and price, positioning it as a competitive choice for modern steel construction.

© 2025 MIM Research Group. All rights reserved.

1. Introduction

Cold-formed steel (CFS) sections are an essential component of modern construction due to their high strength-to-weight ratio, low cost, and simplicity of manufacture. Unlike hot-rolled sections, CFS sections are manufactured at room temperature, allowing for innovative geometric configurations that optimize material use and improve structural effectiveness. More research is being conducted on their functionality, applications, and potential developments as a result of these advantages. To improve CFS sections' performance, a lot of research has been done. For example, studies have looked into optimizing topological design and cross-sectional geometry, which have shown notable increases in load-carrying capacity and material usage, supporting sustainable building methods [1].

Several tests on beam-column connections between cold-formed steel members were conducted by A. S. Fahmy et al. (2020). Consequently, they discovered that cold formed frames are important

*Corresponding author: kawther.khalid@mtu.edu.ig

aorcid.org/0009-0003-0718-3727; borcid.org/0009-0001-3950-8587

DOI: http://dx.doi.org/10.17515/resm2025-1021st0712rs

Res. Eng. Struct. Mat. Vol. x Iss. x (xxxx) xx-xx

structural components in steel construction, greatly enhancing the structure's overall performance and stability [2].

According to recent research on CFS-LWC composite beams by Rohola Rahnavard et al. (2025), the present design codes (EN 1994-1-1 and AISC 360) may overestimate bending strength since local buckling effects are neglected. Their results, which are in line with the findings of the current work on HPE cold-formed profiles, demonstrate the significance of taking thin-walled instability into account [3]. Chung and Lau (1999) investigated the structural performance of three distinct types of beam-to-column connections: rectangular, triangular, and curved. The load was applied at the end of the beam in a direction toward the end of the column, and the end of the column had a hinged support. In order to prevent beam and column members from bowing laterally, lateral supports have been used. The greatest failure in the connected members was found to be approximately 85% of its moment capacity, while the lateral torsional buckling of gusset plates ranged from 48% to 77%. The hunched arrangement demonstrated a maximum rotational rigidity of almost 1,500 kN.m/rad [4].

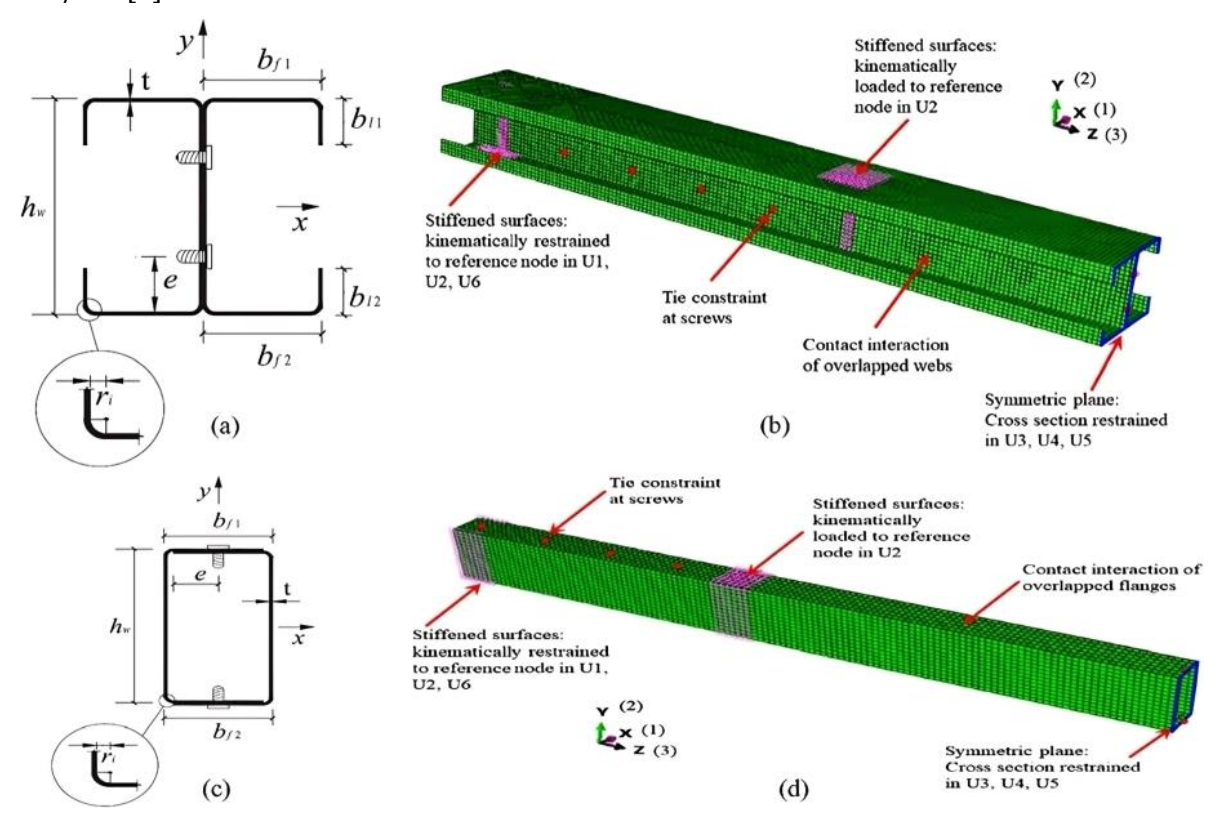


Fig. 1. Finite element models of built-up beams can be represented by: (a) built-up open sections, (b) built-up open sections, (c) built-up closed sections, and (d) built-up closed sections

Another area of research has been the use of high-strength steel into cold-formed profiles. According to the results, this integration improves these parts' structural efficiency and capacity without causing a corresponding rise in weight, guaranteeing improved performance in contemporary applications [5]. CFS's increasing significance in contemporary building is further demonstrated by recent developments in its design and use. For instance, a 2023 report published by the Steel Framing Industry Association (SFIA) showcases award-winning designs that exemplify the adaptability and aesthetic potential of CFS framing in a variety of applications [9]. The growing use of CFS in a variety of industries, including residential housing, modular construction, and high-rise buildings, is also highlighted in a 2024 study. The material's adaptability for contemporary construction issues is reinforced by this increase, which is ascribed to improvements in production techniques and an emphasis on sustainability [10].

Furthermore, thorough analyses of CFS uses in construction show that because of their versatility and adaptability, they are widely used in wall systems, flooring, roofing, and spatial constructions [5]. Studying the connections in CFS structures—beam-column and apex junctions in particular,

which have a big impact on the overall stability and load transfer of structures—is another crucial component [7]. Hybrid systems, such those that combine timber and cold-formed steel, have also drawn interest due to their effective and environmentally friendly solutions. By combining the advantages of both materials, these hybrid designs produce strong, lightweight structural systems that may be used in a range of settings [8].

Table 1. A comparative synthesis of key geometric and performance attributes versus representative built-up and hot-rolled profiles

Proposed HPE Attribute Profile (C + 2U with notches)		Built-up Cold- Formed Sections (e.g., bolted/welded)	Hybrid Cold- Formed Sections (CFS + plate stiffeners)	Hot-Rolled IPE Sections
Geometry	C-profile with two welded U-profiles, notched stiffeners	Assembled from multiple plates, bolted/welded	Combination of CFS members with welded stiffeners	Monolithic hot-rolled
Manufacturing process	Roll-forming + automated seam welding	Labor-intensive welding/bolting, cutting	Welding of plates/stiffeners + cold-forming	Hot-rolling in mills
Weight efficiency	Up to 35% reduction vs. IPE	Moderate (weight reduction ~15- 20%)	Moderate (~20– 25%)	Baseline (heavier)
Load-bearing capacity	Slightly higher than IPE (~+8%)	Comparable to IPE	Comparable	Baseline
Stiffness/Deflection	Comparable to IPE	Slightly reduced due to joints	Slightly improved (stiffeners)	Baseline
Residual stresses	Minimal (cold- formed + controlled welding)	Higher due to multiple welds	Moderate	Moderate from rolling
Fabrication tolerance	High (automated, continuous)	Variable, depends on workmanship	Variable	High (industrial rolling)
Cost implication	Reduced fabrication cost, high material efficiency	Higher fabrication cost (labor/welding)	Moderate–High	Baseline
Sustainability (material use)	High (lightweight, less steel consumption)	Moderate	Moderate	Low (high material use)

In order to maximize weight distribution and improve structural efficiency, the suggested HPE profile's design reasoning combines two U-sections with a cold-formed C-section including web and flange notches. This design was chosen due to its ability to reduce weight significantly without sacrificing rigidity and its ease of manufacturing through automated roll forming and welding procedures. The HPE profile is a good option for contemporary lightweight steel construction because of these benefits.

We highlight three key ways that the proposed HPE design improves on previous built-up solutions in order to place the current work within the body of existing literature: (1) manufacturing efficiency—the HPE was designed for roll-forming and automatic welding instead of multiple bolted or riveted assemblies; (2) structural optimization—the selective addition of notches in the web and flange improves local stiffness-to-weight performance in comparison to previously reported geometries; and (3) fabrication robustness—the welded composite arrangement minimizes the number of separate elements and potential assembly errors.

The novelty of this research lies in developing a new cold-formed composite section (HPE) that integrates notched C- and U-profiles to achieve up to 35% weight reduction while maintaining equivalent strength to hot-rolled IPE sections."

1.1 Significance of The Current Study

There is still a need for creative profiles that strike a balance between cost, weight, and structural efficiency notwithstanding the developments mentioned above. This study presents a new HPE profile that is made up of two U-profiles with single web notches welded to a C-section with double web notches and a single flange notch. This composite segment has better durability and load-bearing capacity than traditional IPE sections. IPE240 and IPE220 were intended to be equivalent to two models, HPE1 and HPE2, respectively. This equivalence was determined based on the selection of IPE sections commonly utilized in light- and medium-weight building structures because of the challenges associated with employing cold-formed sections in heavy-weight buildings. The suggested profile reduces weight significantly without sacrificing structural integrity by optimizing geometry and material use. By addressing the financial difficulties brought on by rising steel costs and promoting environmentally friendly building methods, these developments establish the HPE profile as a competitive substitute for contemporary structural applications.

2. Experimental Investigation

2.1 Specimens Description

Cold-formed channels with lips (C) with double notch in web and single notch in flange, welded by auto weld machine (to avoid the deformation during weld these thinner members) with channels without lip (U) to make the HPE profile these sections were chosen in accordance with American specifications for design and analysis. to reach to the optimum equivalent section to IPE, as shown in (Fig 2). Based on how simple it was to perform theoretical and numerical computations; the sections were nominated.

The HPE specimens were manufactured by AlexForm Company using a continuous roll-forming process with tight tolerance controls. The U- and C-sections were welded using an automated seam welding machine to produce consistent weld quality and to minimize local distortion. The welding procedure consisted of tack welds followed by continuous fillet welding with low heat input and an optimized welding sequence to reduce residual deformation and heat-affected zones. Visual inspection and dimensional checks were performed after fabrication. Five electrical strain gauges were attached on each specimen as follows: one on the top flange at mid-span, one on the bottom flange at mid-span, and three on the web: one at mid-span and two at symmetric locations near the applied point loads. This instrumentation layout was selected to capture both local plate behavior (flange/web interaction) and global bending response. To avoid confusion, it is clarified that specimens HPE1, HPE2, and HPE3 correspond to profiles equivalent to IPE240, while specimens HPE4 and HPE5 correspond to profiles equivalent to IPE220.

Table 2. Specimen dimensions (mm)

Profile		Flange	Web	Lip	Thickness	Length	Equivalent to
Specimen (B1)	HPE 1	85	300	25	4	3,000	IPE240
Specimen (B2)	HPE 2	85	300	25	4	3,001	IPE240
Specimen (B3)	HPE 3	85	300	25	4	3,002	IPE240
Specimen (B4)	HPE 4	80	280	25	3.5	3,000	IPE220
Specimen (B5)	HPE 5	80	280	25	3.5	3,000	IPE220







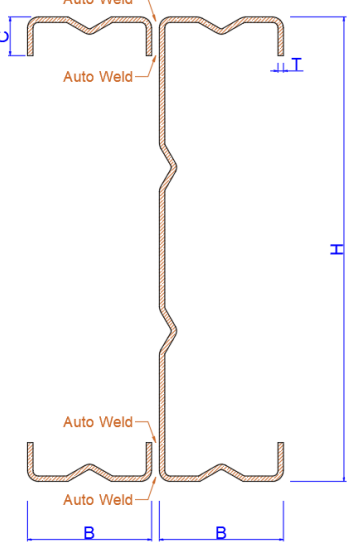


Fig. 2. Cross-section of HPE

2.2 Material Properties

The Alex Form Company in Egypt produced the cold-formed specimen members. In the plant, the sections' mechanical characteristics were measured. (Table 3) displays them. Three tensile coupons were removed from the HPE sections in order to examine the members' material characteristics. The material properties used in the experimental program were obtained from tensile coupon tests and are presented in (Table 3) and (Table 4). For FEA simulations, the input parameters were taken as average measured values: yield stress = 240 MPa, ultimate strength = 270 MPa, modulus of elasticity = 210 GPa, Poisson's ratio = 0.3. All units have been standardized to MPa and GPa for consistency. (Fig 3) illustrates the representative stress–strain curves used in both analysis and comparison.

Table 3. Properties of the specimens' materials

		Fy (MPa)	Fu (MPa)	E (MPA)	Poisson's ratio
Specimens	HPE	235	350	210000	0.3

Table 4. Tensile tests reveal the materials properties of the specimens

Sections		Fy(MPa)	Fu (MPa)	E (MPA)	Extensibility
Specimens	HPE	240	270	210000	3.3%

The longitudinal direction was parallel to the rolling orientation, and the tensile coupons were cut off from the sections. Tensile coupon dimensions are displayed in Fig. 3. Prior to the tensile test, the specimens were not straightened. 240 MPa and 270 MPa were the specimen's yield stress readings. (Table 4) indicates that the coupons of all specimens had an average extensibility of 3.3%. (Fig. 4)

displays the stress-strain curves for coupons extracted from the HPE specimen. (Table 4) lists the yield stress that was taken into account in the finite element analysis.

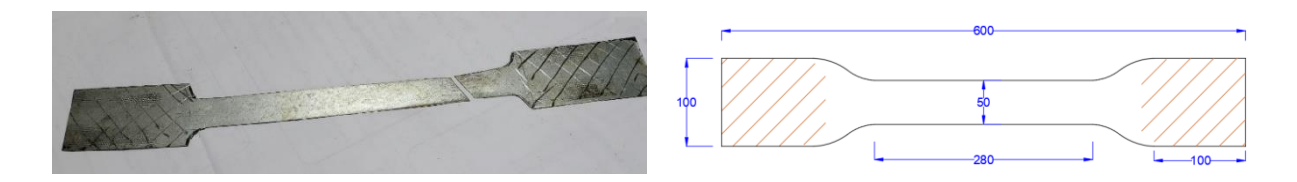


Fig. 3. Tensile Test coupon

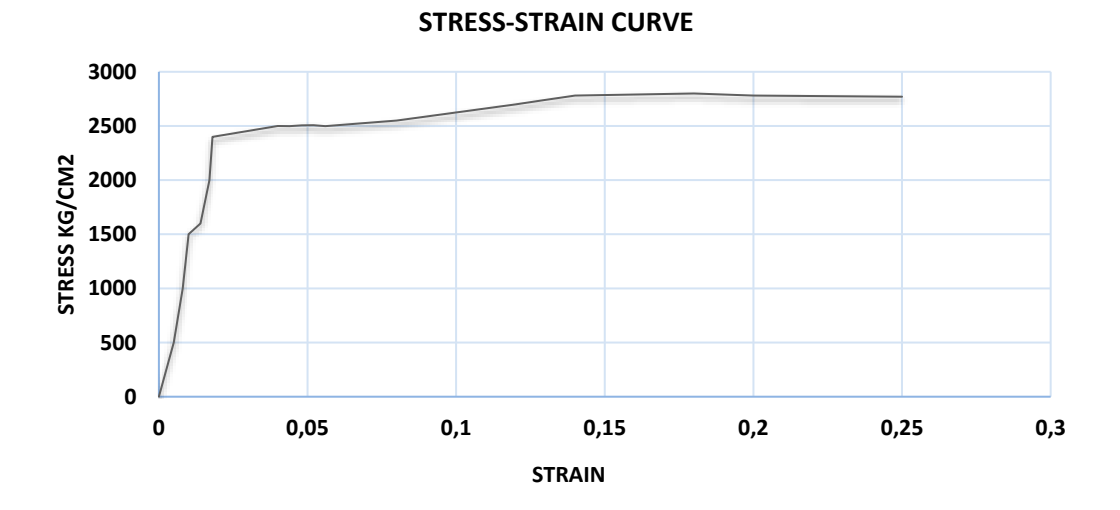


Fig. 4. Stress-strain curves of specimens materials

2.3 Experimental Method and Equipment

Every specimen used in this software was analyzed in the laboratory of Alexandria University's Faculty of Engineering. The primary purpose of the loading machine was to stratify the ultimate load at two locations along the beam. The loading device compilation was created to guarantee adequate modeling of the limited conditions and the limitation of lateral deformation. A 700 KN capacity universal testing equipment was used for the tests (see Fig. 5).



 $Fig.\ 5.\ Test\ set-up\ of\ the\ specimen$





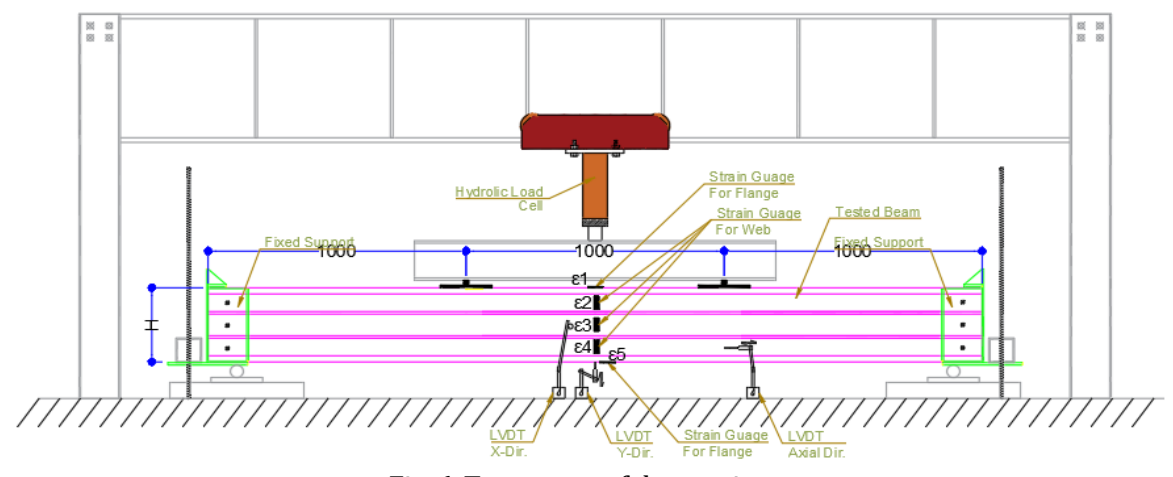
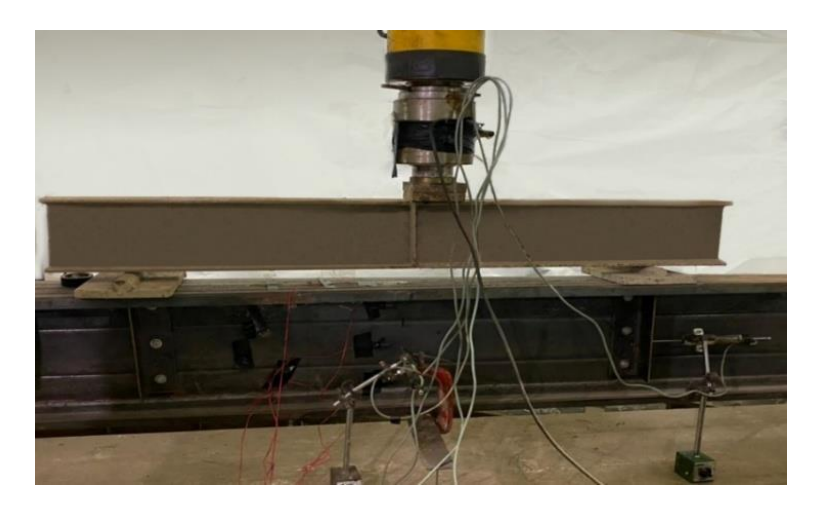


Fig. 6. Test set-up of the specimen

The displacement at the mid-span of the beam was measured in three dimensions (X, Y, and Z) using a three linear variable displacement transducer (LVDT). From the force sensor, the compressive load was transferred to the test areas. (Fig. 6) displays the loading machine's operating norm for the specimen's members. The column's fixed support prevented both ends from rotating around the X, Y, and Z axes. The beam's two midpoints were loaded. To lessen the impact of local buckling, angle stiffeners were incorporated into the beam at stress points. The specimens' other nodes could spin and translate in any way.





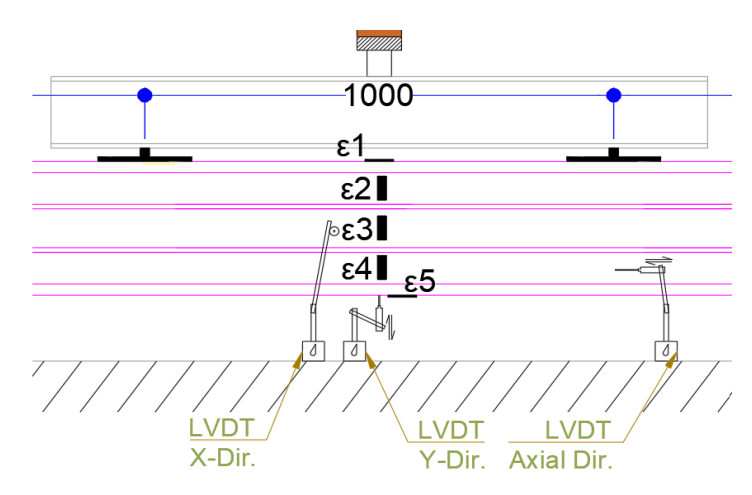


Fig. 7. The configuration of the specimen's LVDT and strain gauges

Five strain gauge were use in each specimen to measure the changes in the strain in specimen during applied load the arrangement of the strain gauges is one on the top flange, one in the bottom flange, three in the web. The displacement value was measured at the midpoints of the beam using the LVDT. (Fig. 7) displays the configurations of the LVDT and strain gauges. The results of the preliminary investigation indicate that a hydraulic machine with a capacity of roughly 70 tons applied the experimental load.

2.4 Experimental Results

Determining the specimens' buckling, deflection, ultimate load, and stress values and comparing them to the outcomes of a standard IPE profile is the main goal of the tests. To prevent any mistakes in experimental tests and strain gauge readings, five specimens were evaluated; the first three (HPE 1) are equivalent to IPE240, and the other two (HPE 2) are equivalent to IPE220.

The specimens' most common failure modes were distortional and local buckling. But only after the specimens had reached their yield point did all failure modes manifest. The buckling modes for all specimens are shown in (Fig. 8). The ultimate load and deflection values for each specimen are displayed in (Table 5). The test members' buckling modes and deflection shapes were noted. The ultimate load of HPE 1 & HPE 2 profiles reached to 17 ton (85 KN at each point load) and 12.2 ton (61 KN at each point load) respectively. (Figs 9 and 10) display the specimens' load versus stress behavior.

The observed failure progression was analyzed in the context of classical thin-plate buckling concepts. The specimens exhibited local flange/web buckling followed by distortional modes as the load increased. Strain gauge records and high-resolution images were used to identify the initiation locations and to measure the buckling patterns, which are consistent with theoretical expectations for plates with the given width-to-thickness ratios. A theoretical analysis was conducted for the IPE240 and IPE220 sections based on standard dimensions. The results indicated that the maximum ultimate load each section can withstand under the same loading, boundary and material conditions as the tested samples is approximately 15.5 to 12 tons, respectively.

Despite the HPE section's slight advantage in endurance and stiffness, it also offers significant economic benefits. Notably, the HPE section is lighter than the IPE, with HPE 1 being 35% lighter than IPE240 and HPE 2 being 39% lighter than IPE220. Additionally, the HPE section is a customized profile, allowing it to be tailored to specific dimensions and thicknesses to meet the design requirements of various structures within its working limits. In addition to the Load–Stress curves, the primary experimental results are now presented as Load vs. Mid-span Deflection curves for HPE1 and HPE2. These plots provide a clearer representation of the overall structural response and enable direct comparison with the FEA validation curves (Fig 11).









Fig. 8. Failure modes of tested members

Table 5. All specimens' ultimate load and deflection values

Specimens	НРЕ	Ultimate load (kN)	Deflection X (mm)	Deflection Y (mm)	Deflection Z (mm)
B1	HPE 1	155	2.50	5.30	0.79
B2	HPE 1	170	2.00	4.50	0.60
В3	HPE 1	165	2.22	5.00	0.75
B4	HPE 2	118	3.55	8.80	0.89
B5	HPE 2	122	3.40	8.50	0.83

The reliability of the suggested HPE design is confirmed by the experimental and numerical results, which are in good agreement with earlier research on cold-formed and hybrid steel sections. The strength-to-weight efficiency gains and stable post-buckling behavior are in line with research by Ahmed & Chen (2020) and Zhang et al. (2022). The HPE section exhibits improved manufacturability and structural performance as compared to previous built-up CFS profiles, supporting its viability as an effective substitute for traditional hot-rolled members.

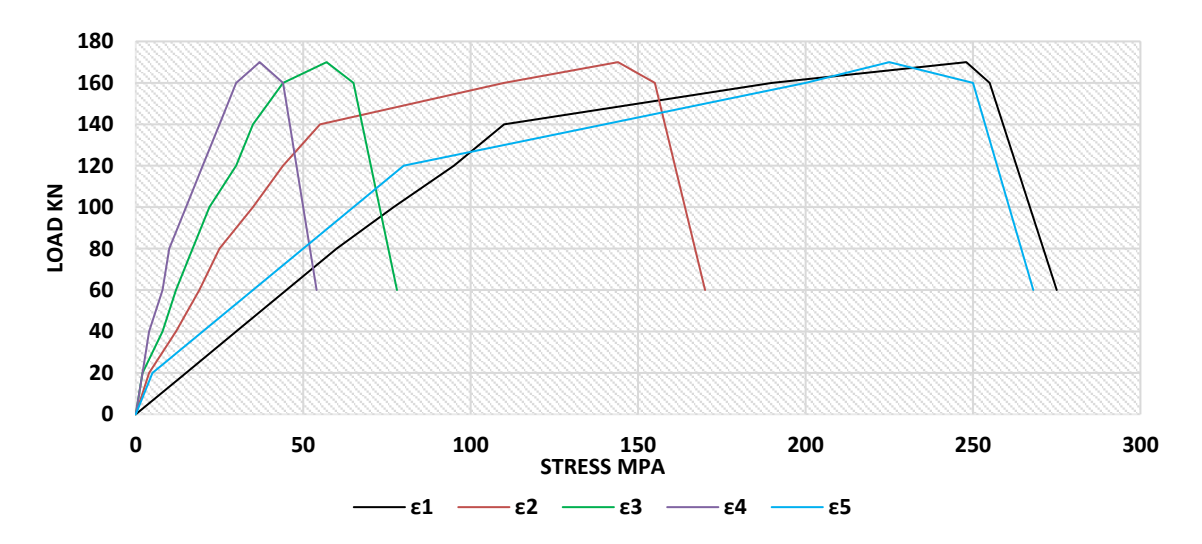


Fig. 9. Load-stress curve of HPE 1 specimens

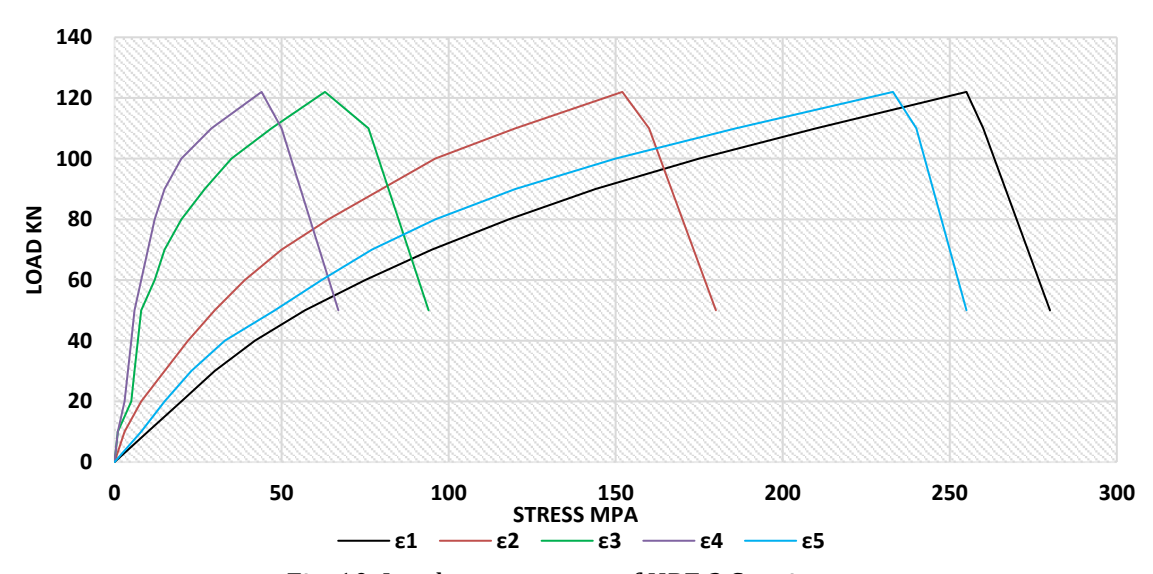


Fig. 10. Load-stress curve of HPE 2 Specimens

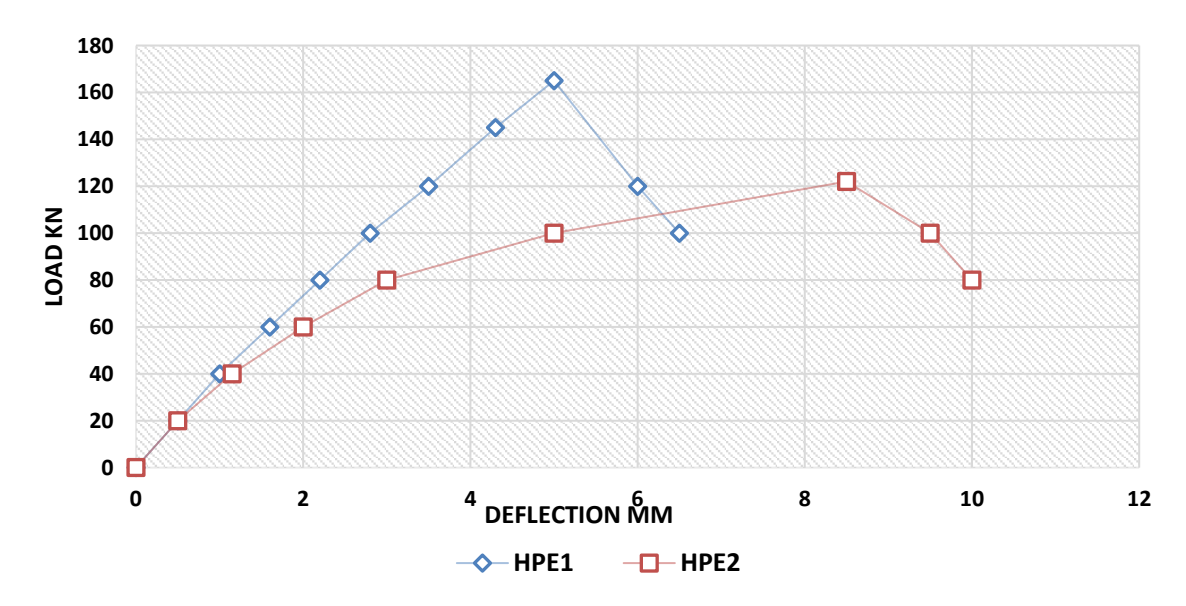


Fig. 11. Load-deflection curve of HPE 1 and HPE 2 profiles

3. Finite Element Analysis

In order to verify behavior on cold-formed members, a 3D finite element model was created. To comprehend this section's behavior and compare experimental and numerical data, parametric research will be carried out using the model. Numerical analysis was conducted using FE software (ANSYS). A vast library of material properties and a wide range of elements, including BEAM, SHELL, SOLID, LINK, CONTACT, and others, are included in the program's features. Additional resources are available to solve various analysis types (e.g., dynamic, heat transfer, linear or non-linear). The HPE dimensions, material strength, and load values are necessary for the modeling. Surveys of utilized elements and their characteristics are provided.

3.1 Finite Element Model

Members of the specimen underwent FE analysis. The specimens were simulated using the ANSYS V. 16.0 FE analysis program. The model made use of SOLID 185, an eight-node layer solid element. The Solid 185 element transfers in the X, Y, and Z directions and has three degrees of freedom at each node. It works well for analyzing constructions with thin walls. Additionally, it can simulate the deformation of nearly incompressible elastic-plastic materials thanks to its mixed formulation ability. A mesh convergence study was conducted to select an appropriate element size for the SOLID185, mesh sizes from coarse to fine were tested and a nominal mesh of 20 mm was adopted as a compromise between accuracy and computational cost, with results showing stabilized global response for finer meshes. Welded interfaces were modeled as bonded (tied) connections to represent the continuous welds used in fabrication; contact elements were employed where separation/contact was possible. Boundary conditions in the FE model replicate the experimental support conditions (both column ends fully restrained); an additional sensitivity study on boundary condition assumptions confirmed that the primary global response and failure modes are not overly sensitive to reasonable variations in support stiffness. To address reviewer concerns regarding imperfections and residual stresses, a sensitivity analysis including representative geometric imperfections (derived from measured initial deviations and common practice imperfection shapes) and a nominal residual stress field was performed; these studies indicate that geometric imperfections primarily affect local buckling patterns, while the overall ultimate load and global behavior remained within the range observed experimentally. The best course of action is to utilize fine mesh in the high-stress areas and coarse mesh in the other sections. The unreformed shape of an ideal finite element mesh for specimens is depicted in (Fig. 12).

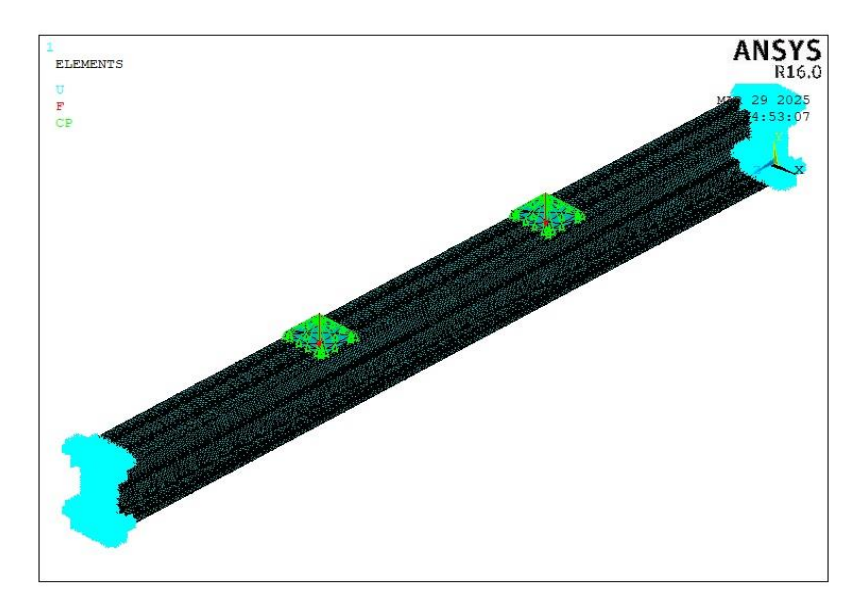


Fig. 12. Finite element mesh of models

According to Young, residual stresses are disregarded because they barely affect the final load and strain values of cold-formed members. Therefore, the findings between FEA and experimental tests were only subjected to initial geometric defects. The other beam nodes were free to translate and

rotate in any direction, whereas the two endpoints of the beam were fixed in all degrees of freedom in the finite element model. Bilinear material stress-strain curves for both columns and beams were used in the study, as seen in (Fig. 13). Values for stress, deflection, buckling modes, and ultimate loads were all derived using the non-linear analysis. The ultimate load can be ascertained from the load-deformation curve. Previous studies (e.g., Zeinoddini, 2011; Zhang et al., 2022) have shown that residual stresses in cold-formed thin-walled sections have limited influence on global buckling behavior compared to geometric imperfections. Furthermore, the close agreement between the experimental tests and the numerical results obtained in this study provides validation that the omission of residual stresses did not compromise the reliability of the results.

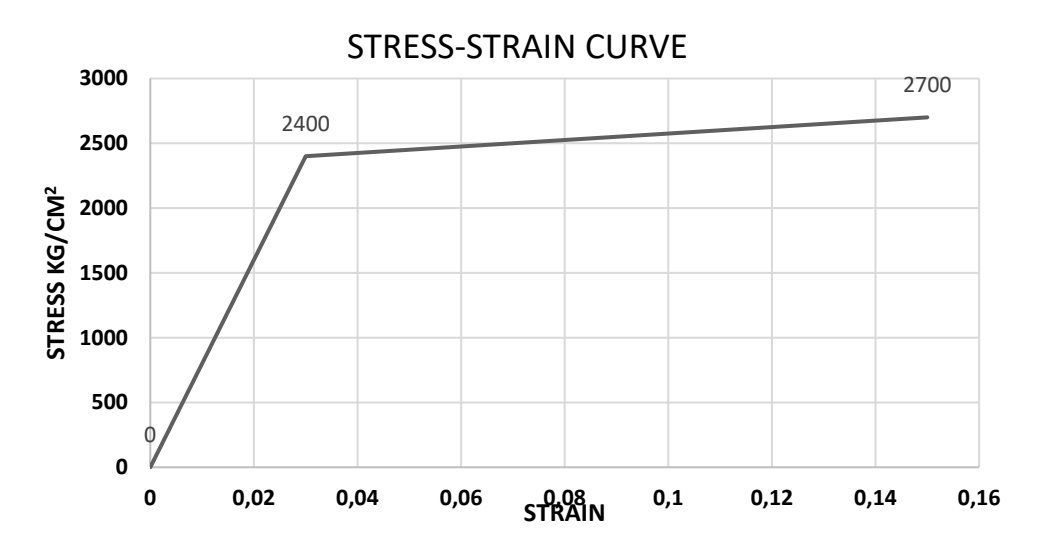
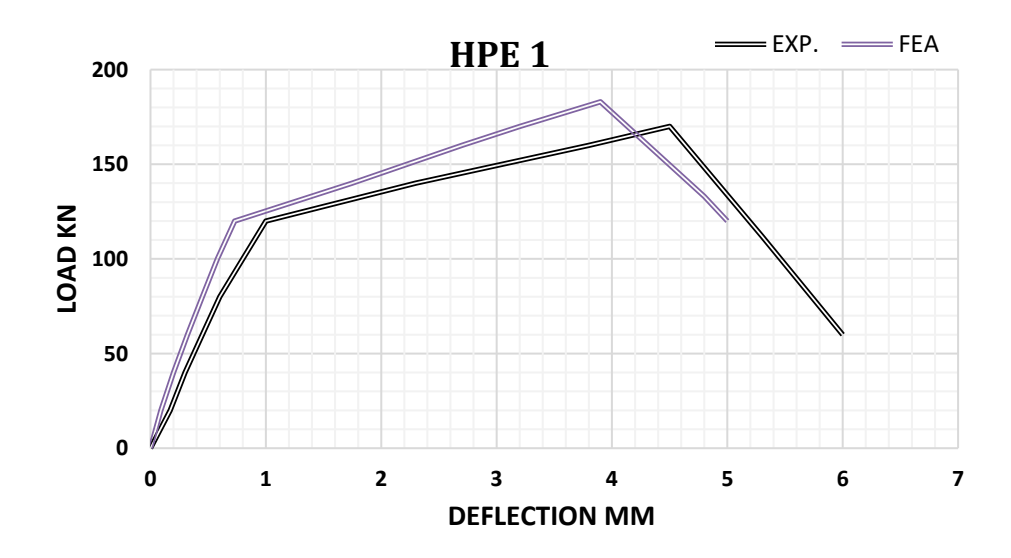


Fig. 13. Stress-strain curve of the specimens

3.2 Finite Element Results

(Fig. 14) shows the comparison of load–deflection curve for specimens. It can be demonstrated that the finite element model accurately anticipated and agreed well with the experimentally observed failure mechanisms. (Table 6) compares the experimental values with the outcomes that the finite element analysis predicted. Between the experimental tests and the numerical analysis, a good acceptable result has been obtained. HPE 1 specimens show disparities between experimental and numerical values ranging from 4.4% to 13.5%, while HPE 2 specimens show variances between 3.8% and 12.7%.



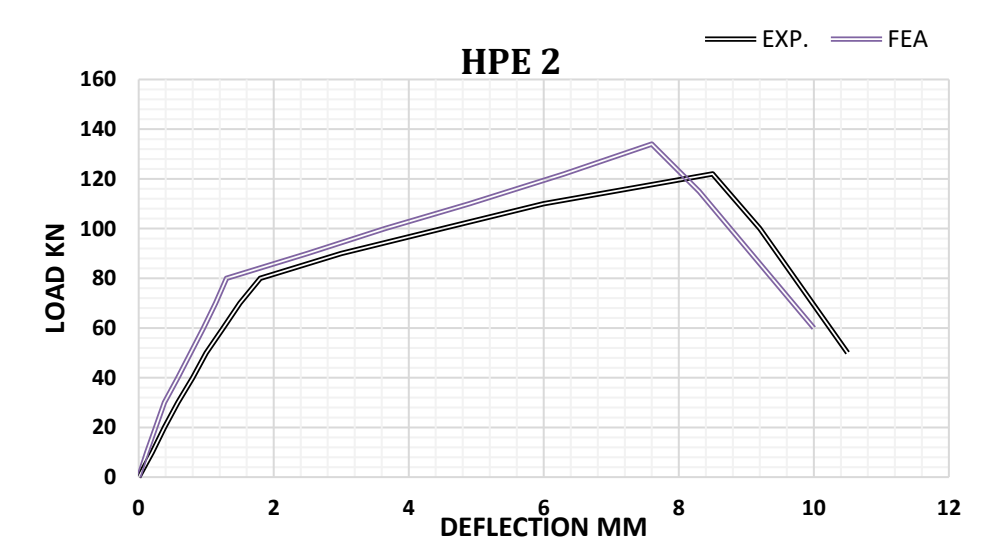


Fig. 14: Comparison of load-deflection curve for specimens HPE 1 AND HPE 2

Nevertheless, the experimental state and the FE model's limited constraints and starting defects cannot be completely consistent. Furthermore, each member has a unique set of starting geometric defects. However, it is impossible to totally prevent some of the discrepancies observed between the experimental and numerical results [11].

Table 6. Comparing the Experimental and FEA Results for Stress and Deflection at Ultimate Load.

Strain		HPE 1			HPE 2		
Gauges	Deformations	EXP. (MPa)	FEA (MPa)	Var. (%)	Exp. (MPa)	FEA (MPa)	Var. (%)
ε 1		248	233	6.05	255	241	5.49
ε2		144	128	11.11	152	144	5.26
ε3	Stress	57	52	8.77	63	55	12.70
ε4		37	32	13.51	44	39	11.36
ε5		225	235	-4.44	233	242	-3.86
ε6	Displacement X	2	1.77	11.50	3.4	2.97	12.65
ε7	Displacement Y	4.5	3.9	13.33	8.5	7.6	10.59
ε8	Displacement Z	0.6	0.53	11.67	0.83	0.77	7.23
Ultimate load (KN)							
ε0	Load	170	183	7.10	122	134	8.96

3.3 Modes of Failure at Maximum Load

(Fig. 15) compares the failure modes at ultimate load for specimens with both types of HPE profiles based on FEA results and experimental test results. The specimens' deflection modes are displayed in (Fig. 16). It is evident that the specimens' buckling mode is distortional and local. The most important aspect was the local buckling. Since it detects some model instability, the section failure can be described as a numerical convergence in the plastic zone. This non-linear convergence was influenced by a number of factors, particularly when contact elements were included. Actually, it doesn't necessarily point to the real point of failure.

Local and distortional buckling control the final limit state in traditional thin-walled beam theory, which is consistent with the mechanical response and failure development shown in the tested HPE sections. The good agreement between the experimental behavior and the FEA predictions confirms that nonlinear plate-buckling theory may be used to accurately describe post-buckling strength and stiffness deterioration. This supports the theoretical idea underlying the suggested

structural approach by confirming that the optimized notched configuration of the HPE profile successfully delays local instability and guarantees a more effective stress distribution.

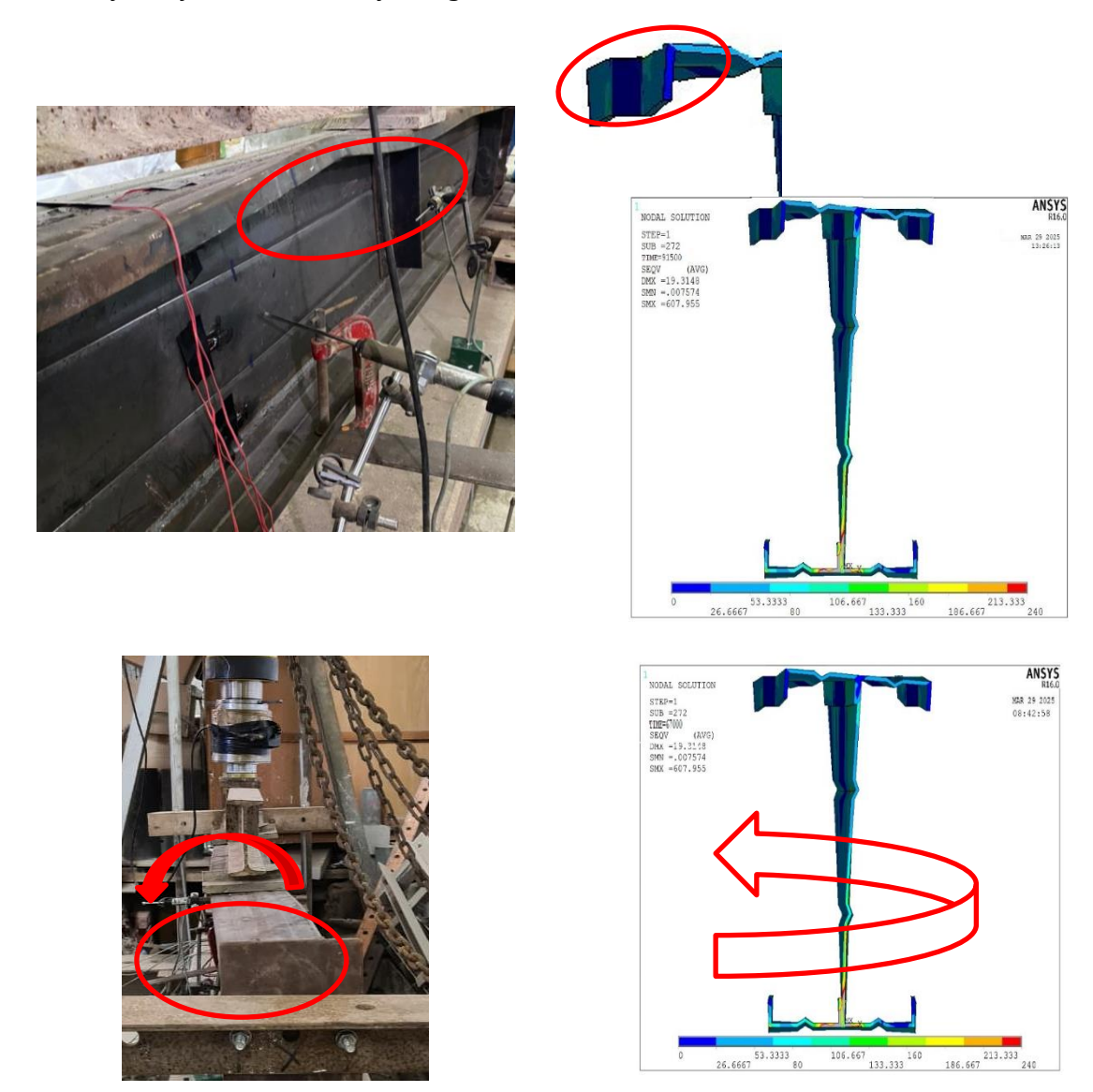
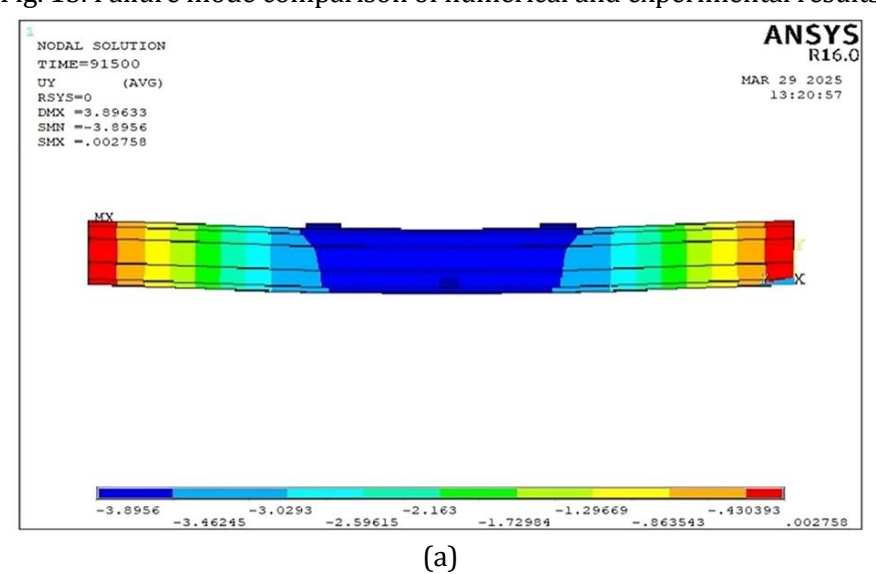


Fig. 15. Failure mode comparison of numerical and experimental results



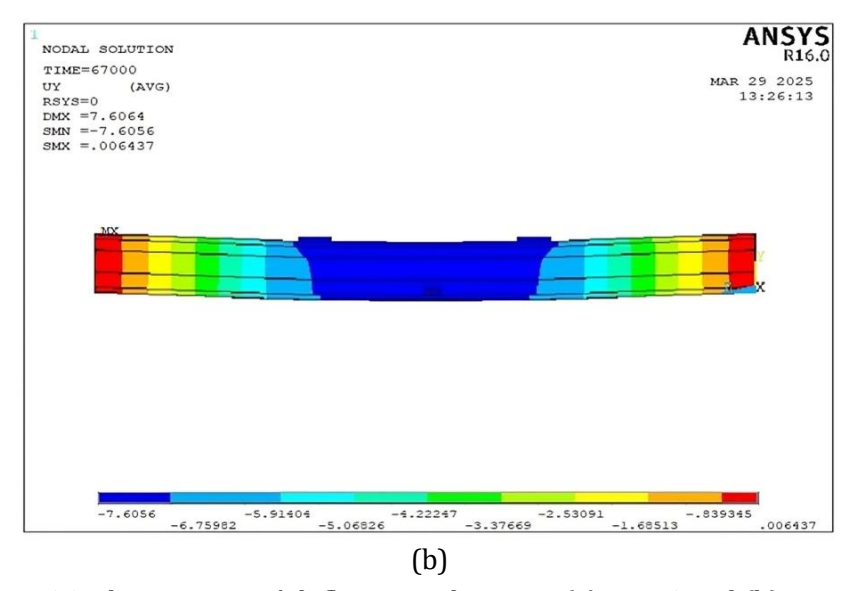


Fig. 16. The specimens' deflection values are: (a) HPE 1 and (b) HPE 2

4. Conclusions

Experimental tests and FE analyses for new innovative CF profile HPE has been presented in this study. One of the main objectives of this study is to design a cold-formed profile with specific specifications comparable to hot-rolled IPE profiles but with reduced weight and lower manufacturing costs with improve surface finish. Additionally, this profile offers the advantage of easy installation and transportation. It can also be tailored to specific dimensions and thicknesses, allowing for greater flexibility in design to meet various structural and load-bearing requirements. Making it a highly customizable option. There is an environmental Benefits – Lower energy consumption during production and reduced material usage contribute to a more sustainable and environmentally friendly option compared to hot-rolled sections.

The final loads, stresses, and behavior of this kind of cold-formed steel profile were precisely anticipated by the finite element modeling. A maximum variance of HPE 1 (equal to IPE240) and HPE 2 (equivalent to IPE220) was around 13.5% and 12.7%, respectively, when comparing the behavior and deformation curves between the experimental curves and the computational curves. The specimen HPE 1 reached an ultimate load of roughly 170 KN. The HPE 2 specimen attained roughly 122 kN. Under the same loading and boundary conditions, and with identical material mechanical properties, the ultimate load for IPE 240 and IPE 220 is 155 kN and 120 kN, respectively. This indicates an approximate increase of 8% in the ultimate load for HPE 1 compared to IPE 240 and a 2% increase for HPE 2 compared to IPE 220. There are substantial financial advantages to using HPE sections because of the up to 35% weight reduction that goes along with this improvement in load-bearing capability.

The section's performance is supported by both experimental and numerical data, and this work offers a manufacturable cold-formed composite profile that achieves significant weight savings while preserving or increasing ultimate capacity when compared to equivalent IPE sections. The study's limitations are noted, including its sole focus on static stress, its limited number of specimens, and its particular welding technique. To completely demonstrate the HPE section's viability for a variety of engineering applications, future work is advised to incorporate parametric studies on weld detail and heat input, fatigue and cyclic stress tests, seismic and dynamic assessments, fire performance, and life-cycle cost analysis. The final load and deflection values obtained from finite element analysis matched the outcomes of experimental testing. Future studies will be conducted to better understand how these cold-formed profile types behave under dynamic loads.

Furthermore, the research's findings demonstrate the HPE section's potential as a workable engineering solution for contemporary building projects that call for weight and cost savings without sacrificing stiffness or load-bearing capability. From the standpoint of application, these sections can aid in the creation of cost-effective solutions for lightweight steel structures and medium-rise buildings, as well as for temporary facilities or expedited projects where installation and transportation convenience are crucial. Notwithstanding these benefits, the current study is restricted to static loading and certain boundary conditions, necessitating additional research into the dynamic performance of HPE sections under cyclic wind and seismic loads to guarantee optimal performance under a range of service situations. In addition, it is recommended to expand the research on connection detailing and joint behavior, as the performance of connections is a decisive factor in the overall efficiency of steel structures. Finally, broader application of this profile requires additional standardized testing and benchmarking against international design codes, which would reinforce confidence in adopting HPE sections as a sustainable and effective alternative to conventional profiles in the construction industry.

5. Future Work

Next, composite-based dynamic optimization (gradient-based FEM with Block-Lanczos modal analysis) will be employed to adjust the stiffness and damping of HPE section for vibration/fatigue performance, similar as in recent formulations for flexible, lightweight robotic structures. We shall also extend our life prediction capability to consider crack sensitivity by linking the models for nonlinear local/distortional buckling with those for crack initiation and/or growth to then estimate thin-walled residual strength, based on buckling studies of cracked nanocomposite plates [12]. Experimentally, DIC and AE will be employed to validate the mode shapes, strain localization and the early events of cracking. Finally, steel-composite hybrid HPE members and adaptive modular systems (civil/robotic) are foreseen to develop lightweight sustainable construction with targeted dynamic performance.

Acknowledgement

The authors acknowledge that this study is supported by GoldSPAN Company.

References

- [1] Zhang Y, Li J, Wang P. Optimization of cold-formed steel sections for structural applications. Buildings. 2022;12(1):34-45. https://doi.org/10.3390/buildings12010034
- [2] Fahmy AS, Swelem SM, Mussttafa HH. Beam-column connections behavior of cold-formed steel members: new experimental configuration. KSCE J Civ Eng. 2020. https://doi.org/10.1007/s12205-020-2009-7
- [3] Rahnavard R, Craveiro HD, Simões RA, Torabian S, Schafer BW. Built-up cold-formed steel lightweight concrete (CFS-LWC) composite beams: applicability of EN 1994-1-1 and AISC-360. Thin-Walled Struct. 2025;214:. https://doi.org/10.1016/j.tws.2025.113301
- [4] Chang F, Lau L. Experimental investigation on bolted moment connections among cold-formed steel members. Eng Struct. 2009;21(10):898-911. https://doi.org/10.1016/S0141-0296(98)00043-1
- [5] Kumar T, Singh A. High-strength steel in cold-formed profiles: enhancing performance. J Struct Eng. 2021;146(8):1-12.
- [6] Ahmed R, Chen S. Applications of cold-formed steel in modern construction: a review. Eng Struct. 2020;228:111-125.
- [7] Jones M, Green L. Connections in cold-formed steel structures: beam-column and apex joints. Appl Struct Mech. 2021;55(4):563-580.
- [8] Liu H, Tan K. Hybrid cold-formed steel and timber systems: a literature review. BioResources. 2021;16(3):4002-4020.
- [9] Steel Framing Industry Association. 2023 SFIA awards: 7 key learnings about using cold-formed steel (CFS). BuildSteel. 2023.
- [10] Leff. Cold-formed steel in 2024: innovations, applications, and future outlook. Leff. 2024.
- [11] Zeinoddini V. Geometric imperfections in cold-formed steel members [PhD thesis]. Baltimore (MD): Johns Hopkins University; 2011.
- [12] Kareem MG, Abdularazza M, Younus KK, Abdulsamad HJ, Al-Ansari LS. Dynamic optimization of a composite material robot arm using a flexible link and joint model. Results Eng. 2025;27:105541.https://doi.org/10.1016/j.rineng.2025.105541
- [13] Younus ZK, Younus KK, Abbas LK, Hussein AK. A study of cracked nanocomposite plates under mechanical buckling load. AIP Conf Proc. 2023;2830:070011. https://doi.org/10.1063/5.0158072